HOKKAIDO UNIVERSITY

Title	Phase-dependent output of scattering process for traveling breathers
Author(s)	Teramoto, Takashi; Ueda, Kei-Ichi; Nishiura, Yasumasa
Citation	Physical Review E, 69, 056224 https://doi.org/10.1103/PhysRevE.69.056224
Issue Date	2004-05-27
Doc URL	http://hdl.handle.net/2115/5429
Rights	Copyright © 2004 American Physical Society
Type	article
File Information	PRE69-5pdf.pdf

Instructions for use

Hokkaido University Collection of Scholarly and Academic Papers : HUSCAP

Phase-dependent output of scattering process for traveling breathers

Takashi Teramoto,* Kei-Ichi Ueda,† and Yasumasa Nishiura
Meme Media Laboratory, Hokkaido University, Sapporo 060-0813, Japan;
Department of Mathematics, Keio University, Yokohama 223-8522, Japan;
and Research Institute for Electronic Science, Hokkaido University, Sapporo 060-0812, Japan
(Received 30 November 2003; published 27 May 2004)

Scattering process between one-dimensional traveling breathers (TBs), i.e., oscillatory traveling pulses, for the complex Ginzburg-Landau equation (CGLE) with external forcing and a three-component activator-substrate-inhibitor model are studied. The input-output relation depends in general on the phase of two TBs at collision point, which makes a contrast to the case for the steady traveling pulses. A hidden unstable solution called the scattor plays a crucial role to understand the scattering dynamics. Stable and unstable manifolds of the scattor direct the traffic flows of the scattering process. A transition point of the input-output relation in a parameter space such as from preservation to annihilation corresponds to when the orbit crosses the stable manifold of the scattor. The phase dependency of input-output relation comes from the fact that the profiles at collision point make a loop parametrized by the phase and it traverses the stable manifold of the scattor. A global bifurcation viewpoint is quite useful not only to understand how TBs emerge but also to detect scattors. It turns out that the scattor for the CGLE (respectively the three-component system) becomes an unstable time-periodic (respectively stationary) solution.

DOI: 10.1103/PhysRevE.69.056224 PACS number(s): 82.40.Bj, 68.35.Fx, 82.20.Wt, 89.75.Kd

I. INTRODUCTION

Spatially localized moving objects such as pulses and spots form a representative class of dynamic patterns in dissipative systems. A qualitative change for the pattern may occur either by interaction with other patterns through collision or due to intrinsic instabilities such as splitting and destruction by itself [1–5]. There is a variety of collision process for particlelike patterns in dissipative systems even restricted to head-on ones [6–14]. A key issue is to classify the input-output relation before and after collision and clarify its underlying mechanism for the scattering process. One of the difficulties comes from the large deformation due to strong interaction. A new viewpoint was presented to clarify the process of head-on collisions among traveling pulses and spots [15,16]: especially a notion of "scattor" was introduced to understand the input-output relation. The scattor itself is just an unstable steady or time-periodic solution (i.e., saddle) and its center of mass does not move, however once there occurs collision, the solution deforms significantly and approaches a part of the unstable manifold of the scattor and is driven by it. The final output is therefore determined by the destination of the unstable manifold. Scattors are in general highly unstable and a variety of outputs originates from those of destinations of unstable manifolds. In Ref. [15] we used the terminology "separator" instead of scattor, however scattor may be appropriate especially for higher codimension case [16].

The issue is reduced, to some extent, to finding the scattors and their dynamic behaviors along unstable manifolds, however it is in general difficult to detect a scattor even by numerics, since it is not an attractor. To overcome this difficulty, the following observation turns out to be quite useful [15,16]: when parameters are close to a transition point where input-output relation changes qualitatively, the orbit becomes very close to the scattor by adjusting an appropriate number of parameters. Once a scattor is obtained at some particular point, then it can be continuated to other parameter regions by using, for instance, AUTO software [17]. The aim of this paper is to study the scattering process for the oscillatory-propagating pulses for the complex Ginzburg-Landau equation (1) with a parametric forcing term [18–21] and the three-component activator-substrate-inhibitor model (3). Since such pulses vary time periodically, the input-output relation in general depends on the phase at collision, which makes a sharp contrast with the nonoscillatory case. It turns out that the scattor for the Complex Ginzburg-Landau equation (CGLE) (respectively the three-component system) becomes an unstable time-periodic (respectively stationary) solution. Our goal is to show the existence of such scattors numerically and clarify the phase dependency of the input-output relation. In what follows we use the terminology "traveling breather"(or TB in short) for the oscillatory-propagating pulse.

Our first model system is the following CGLE with a parametric forcing term [18–21]:

$$W_t = (1+ic_0)W + (1+ic_1)W_{xx} - (1+ic_2)|W|^2W + c_3\overline{W}, \tag{1}$$

where c_0, c_1, c_2, and c_3 are real parameters. The last complex conjugate term represents an external forcing with almost double the natural frequency and $c_2 - c_0$ stands for the fre-

*Present address: Department of Photonics Material Science, Faculty of Photonics Science and Technology, Chitose Institute of Science and Technology, Chitose 066-8655, Japan.

†Present address: Research Institute for Mathematical Sciences, Kyoto University, Kyoto 606-8502, Japan.

 ©2004 The American Physical Society

quency misfit. Equation (1) becomes bistable in an appropriate parameter region where there exists a pair of stable homogeneous states W_0 and $-W_0$. When c_3 is large, the stationary front connecting W_0 to $-W_0$ is stable. Note that the magnitude of $1-|W|^2$ (or the modulus $|W|$) is localized in space, so we call it a pulse rather than a front (or domain wall) in the sequel. It was shown by Coullet *et al.* [19] that Eq. (1) undergoes a supercritical drift bifurcation of the stationary pulse as c_3 is decreased, i.e., Ising-Bloch bifurcation with other parameters being fixed as $c_0=0.10$, $c_1=-0.10$, and $c_2=0.15$. Since it is supercritical, the velocity of bifurcating steady traveling pulse is small near the onset and the two pulses repel each other, therefore the input-output relation becomes preservation. In a slightly different parameter setting such as $c_0=-0.15$, $c_1=-0.10$, and $c_2=0.10$, Ohta *et al.* [20] found a transition from preservation to annihilation as c_3 is decreased. This transition can be understood in such a way [16] that the orbit crosses the stable manifold of the scattor of codim 1 at the transition point and the orbits are sorted out according to which side of the stable manifold it belongs. Scattors are in general highly unstable [15,16], and hence not visible just by solving the evolutions, however, as will be shown below, they can be detected in a systematic way by using AUTO. The local dynamics around the scattor and global behaviors of their unstable manifolds are the keys to link input to output during the scattering process. Moreover such a saddle is not necessarily a steady state, in fact we will see in the sequel that an unstable time-periodic solution plays a role of scattor for TB. In order to have a TB, we employ here a particular set of parameters $c_0=1.0, c_1=-0.5, c_2=1.1$ and take c_3 as a bifurcation parameter in the bistable regime. It is easy to see $\pm W_0=\pm 1$ for this setting. The Neumann boundary condition (zero flux) is imposed and we set to $\Delta x=0.5$ and $\Delta t=10^{-3}$ and the system size is 64. There exist other parameter regions in which traveling breathers are observed, for instance, Mizuguchi and Sasa [21] employed $c_0=1.0, c_1=-0.5, c_2=1.0$ and found a variety of instabilities by computer simulations, however TBs in this regime always annihilate at collision and no transition occurs for the input-output relation. In this paper we investigate the input-output relation of the symmetric head-on collisions for Eq. (1), which is equivalent to considering the collision process with the Neumann wall (see Fig. 1), and reveal the nature of quasi-time-periodic solution as depicted in Fig. 2.

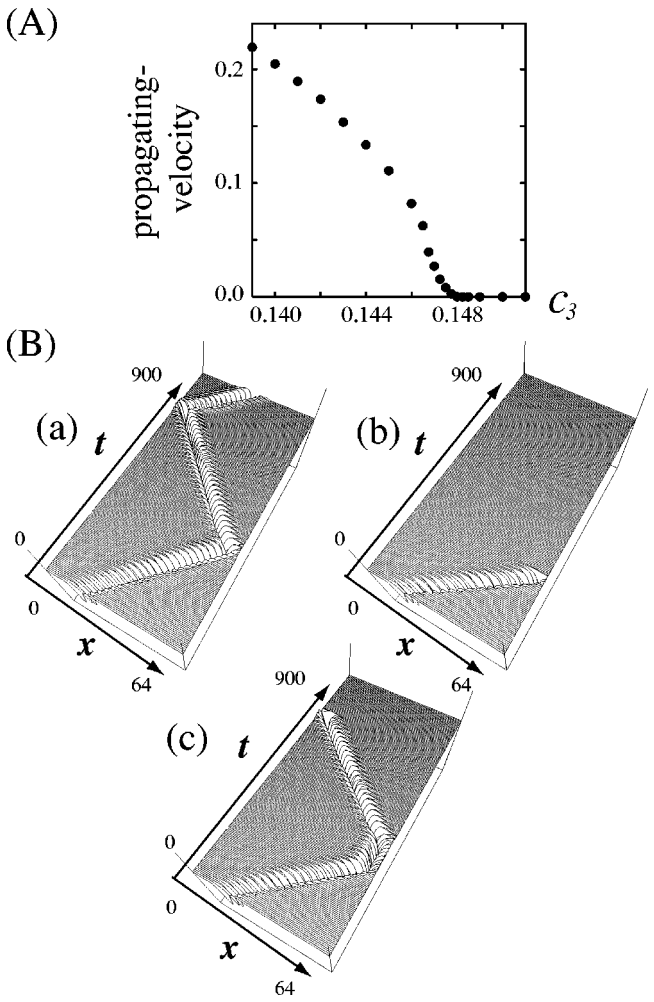

FIG. 1. (A) Long-time average of the propagating velocity as a function of c_3. (B) Transition from reflection to annihilation occurs at $c_3\approx 0.142\,429$ as c_3 is decreased [(a) preservation (reflection) when $c_3=0.144$, (b) annihilation when $c_3=0.140$, and (c) $c_3\approx 0.142\,429$]. The other parameters are set to $c_0=1.0$, $c_1=-0.5$, and $c_2=1.1$. Here we draw the space-time plot of $|W|^2$.

II. ONSET OF TRAVELING BREATHERS AND BIFURCATIONAL ORIGIN OF SCATTORS

As a route to TB from a stationary pattern, two subsequent bifurcations occur, i.e., Hopf and drift bifurcations. For larger $c_3\approx 0.30$, it is easy to obtain a stable stationary pulse as in Fig. 3(A)(a). When c_3 is decreased, a Hopf bifurcation first occurs at 0.230 [see Fig. 3(B)] and the stationary pulse starts to oscillate back and forth, but the center of mass does not move. Slightly away from the Hopf bifurcation point, the oscillations become strongly anharmonic and zigzag shaped. As c_3 is decreased further to 0.148, its center of mass starts to drift as in Fig. 1(A), which indicates the onset of TB. The drift velocity of TB is slow near the onset, since the bifurcation from the standing oscillating pulse to the TB is supercritical as Fig. 1(A). The TB bounces off at the wall, therefore the input-output relation is preservation, namely an incoming TB emits an outgoing TB. When c_3 is decreased to 0.140, the velocity of TB becomes larger, and it annihilates at the collision to the Neumann wall as in Fig. 1(B)(b). It is clear that transition of input-output relation must occur in between 0.140 and 0.148. To detect a scattor near the transition point, orbital behaviors are traced carefully by changing c_3 with keeping the initial condition being fixed. We employ a well-settled TB as an initial data for numerics. Here the "well-settled TB" means that it is obtained after a long-run simulation on a large interval. This makes sense because the concerning TB is asymptotically stable. It turns out that the orbit stays very close to a quasi-time-periodic state for certain time when $c_3\approx 0.142\,429$ as indicated in Fig. 2. A remarkable thing happens as shown in Fig. 1(B)(c), namely the

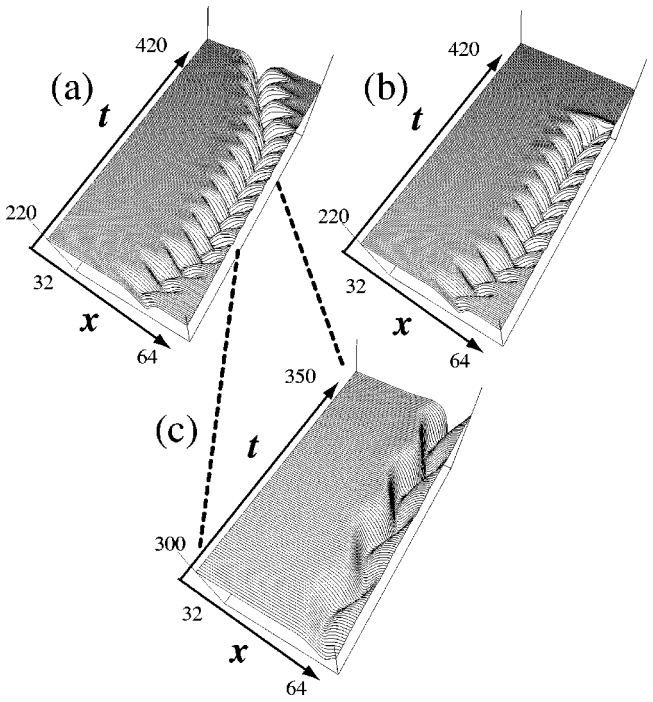

FIG. 2. Magnified figures of transition from reflection (a) to annihilation (b) at $c_3 \approx 0.142\,429$, as c_3 is slightly decreased. (c) A quasi-time-periodic pulse observed at the transition point.

TB is reflected at the first collision, while the annihilation occurs at the second collision despite c_3 being fixed as $\approx 0.142\,429$. This not only makes a sharp contrast with the steady TB case [15,16], but also implies that the bifurcation parameter c_3 is not sufficient to determine the input-output relation. Such a phase-dependent output occurs over a range of c_3 including $0.141-0.143$ and the quasi-time-periodic objects such as Fig. 2 are observed for certain time right after collisions. It indicates the existence of a c_3-parameter family of unstable time-periodic solutions called scattors and those objects play a role of separatrix and should be responsible for the transition of input-output relations for our system.

Although scattors may be obtained approximately by tuning the parameter c_3, this approach has several drawbacks, for instance, it only works near the transition point of codim 1, and it does not give a precise profile to study the linearized spectrum around it. In what follows we present a more systematic and powerful method to detect scattors based on a global bifurcation viewpoint and clarify the origin of phase-dependent output. To control the phase at collision, we change the distance between the initial pulse and boundary, since it is equivalent to shifting the phase of the initial oscillatory pulse.

First we find stationary solutions for larger values of c_3. Figure 3(A) shows relevant unstable and stable steady solutions confirmed numerically for $c_3 = 0.30$ with the aid of the Newton method. Once the stationary solution has been detected, we compute the branches globally by continuation using AUTO. Following the branch of the stable steady pulses SSP (respectively unstable one denoted by USP), there occurs a saddle-node (SN) bifurcation at $c_3 \approx 0.228\,59$ (respectively $0.223\,75$) as in Fig. 4(a). The profile of the unstable

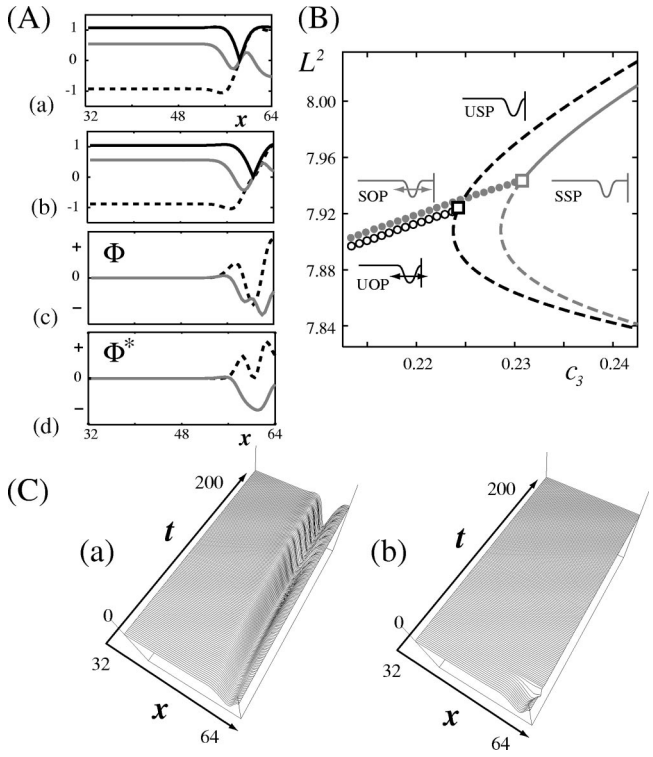

FIG. 3. (A)(a) Stable steady pulse (SSP) when $c_3 = 0.30$; (b) the unstable steady pulse (USP) has only one (real) unstable eigenvalue ($\approx 0.183\,14$) and the associated eigenfunction Φ (respectively its adjoint Φ^*) when $c_3 \approx 0.224\,31$ is depicted in (c) [respectively (d)]. The solid, gray, and broken lines indicate the amplitude $|W|^2$, imaginary, and real parts, respectively. (B) Bifurcation diagram in the neighborhood of the Hopf bifurcation points. L^2 stands for the integral norm of the square of u. The black (respectively gray) line indicates the branch continued from USP (respectively SSP) of (A)(b) [respectively (a)] and black open (respectively gray filled) circles represent the unstable oscillating pulse (UOP) [respectively stable oscillating pulse (SOP)]. (C)(a) [respectively (b)] Response of USP by adding a small positive (respectively negative) constant-multiple perturbation in the direction Φ when $c_3 = 0.227$.

eigenfunction associated with USP denoted by Φ is shown in Fig. 3(A)(c). Note that a Hopf bifurcation occurs supercritically on SSP (respectively USP) near the SN point at $c_3 = 0.230\,75$ (respectively $0.224\,31$) shown as circles in Fig. 4(a). This is the onset of the stable (respectively unstable) standing breather SOP (stable oscillating pulse) [respectively unstable oscillating pulse (UOP)]. The USP has only one real positive eigenvalue even on a whole interval and the associated one-dimensional unstable manifold is connected to the SOP and the homogeneous trivial state, respectively. In fact, taking $c_3 = 0.227$ in between the above two Hopf bifurcation points, and adding a small perturbation proportional to Φ, the output, depending on its sign of the perturbation, is either like Fig. 3(C)(a), i.e., changes into a SOP, or like Fig. 3(C)(b), i.e., a homogeneous state. Actually, besides the USP and SSP branches, there exists another unstable solution branch, however it does not play an important role here, so not shown in these figures. The two Hopf branches SOP and UOP are extended to the range of c_3 in which numerical simulations of Figs. 1 and 2 are carried out. The Neimark-

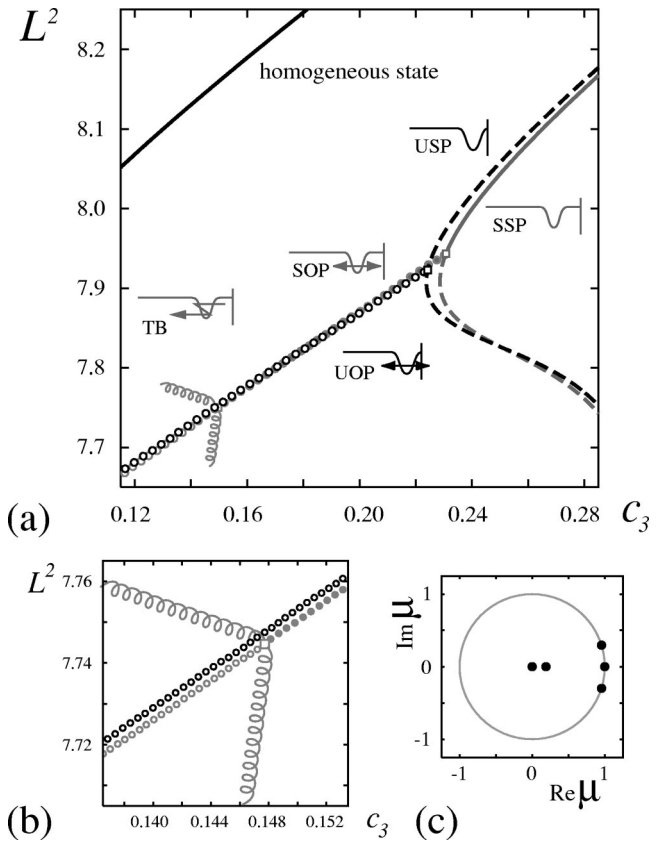

FIG. 4. (a) Global bifurcational origin of the time-periodic scattor. The bifurcation parameter is c_3. The black open (respectively gray filled) circles indicate the unstable oscillating pulse (UOP) [respectively stable (SOP)] connected to USP (respectively SSP). TB emerges below $c_3 \approx 0.148$. The solid line at the top of the figure indicates the stable uniform state. (b) A detail near the NS bifurcation point. (c) The distribution of multipliers μ of SOP at $c_3 \approx 0.148\,022$. The gray circle shows $|\mu|=1$.

Sacker (NS) bifurcation takes place on the stable Hopf branch SOP at $c_3 \approx 0.148\,022$, namely, a pair of multiplier $\mu_{1,2}=0.955\pm 0.297i$ crosses the unit circle as depicted in Fig. 4(c). The Floquet multipliers μ can be used for the criterion of the stability of a periodic orbit. The SOP becomes unstable and the stable oscillatory-propagating pulse, i.e., TB, takes over instead. The c_3 value of the NS point is in good agreement with that of the onset of TB in Fig. 1(A). TBs originate from the NS point of the SOP and we can observe a scattering among them for $c_3 < 0.148\,022$. On the other hand, the UOP is a hyperbolic saddle of codim 1, so that it has only one real unstable multiplier $\mu > 1$. It turns out that the quasi-time-periodic behaviors such as Fig. 2(c) are realized by the UOP. In other words the UOPs are the time-periodic scattors and their unstable manifolds are connected to TBs and the homogeneous state as in Fig. 5.

III. PHASE-DEPENDENT OUTPUTS FROM THE BREATHING SCATTOR

Now we are ready to explain why we have different outputs depending on the phase of collision as in Fig. 1(B)(c).

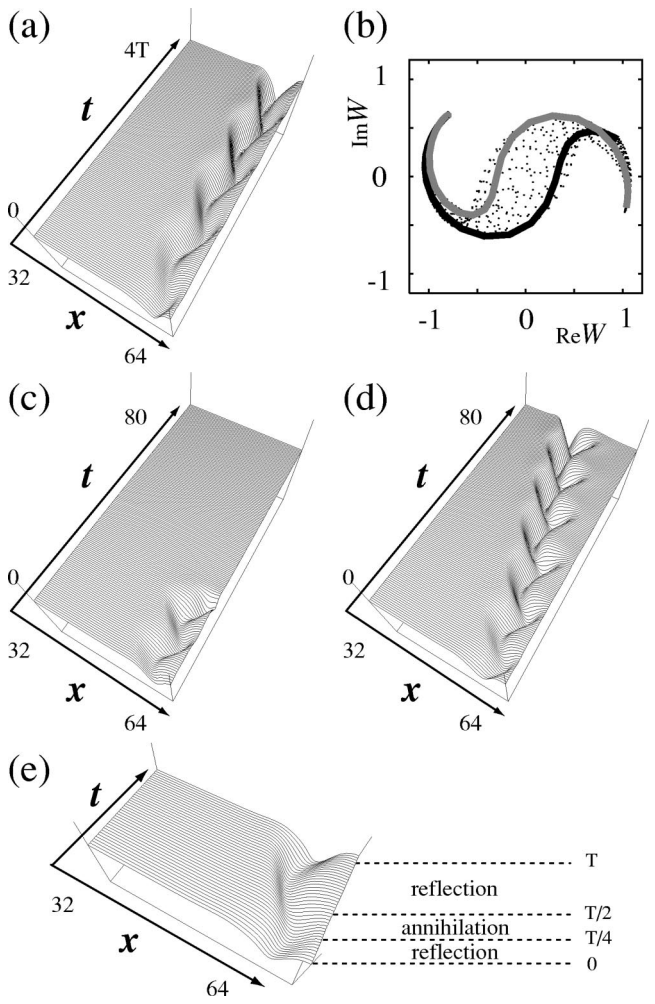

FIG. 5. (a) Spatiotemporal pattern of the scattor with the period $T \approx 12.8730$ at $c_3 \approx 0.142\,429$. (b) Phase portraits of the scattor: The solid (respectively gray) line indicates the interface when $t=3T/8$ (respectively $t=5T/8$). (c) [respectively (d)] Response of the scattor by adding a small constant-multiple perturbation of Φ to the snapshot of the unstable orbit at $t=3T/8$ (respectively $t=5T/8$). (e) Phase-dependent response of the scattor.

We look at the responses of the scattor by perturbing it along the unstable direction when $c_3 \approx 0.142\,429$. To detect the unstable direction theoretically, we have to solve the monodromy operator associated with the linearized operator around the scattor; however, this is not an easy task numerically. We therefore add a small perturbation to each of frames of the periodic orbit in the fixed direction Φ instead, which is generically transversal to the stable manifold of breathing scattor (BS). One period is discretized into 80 frames here. In views of Figs. 5(c)–5(e), the destinations of the unstable manifold are homogeneous state (annihilation), if the perturbation is added to a quarter of the period of the scattor between $T/4$ and $T/2$. Otherwise they are outgoing pulses (preservation).

More quantitatively we can distinguish the behaviors of orbits by calculating the distance between the orbit and the scattor, and its projection along the unstable direction defined as Eq. (2) where Φ^* is the adjoint function of Φ [see Fig. 3(A)(d)]:

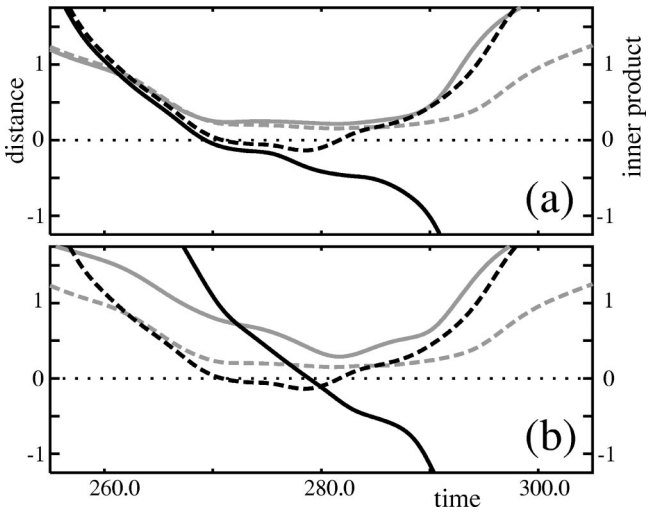

FIG. 6. Time evolutions of the inner product and distance to the scattor. (a) The inner product changes the sign from positive to negative when c_3 is decreased (solid black for $c_3=0.142\,42$ and solid gray for $c_3=0.142\,44$). The associated broken curves represent the distance to the scattor. (b) For an appropriate c_3, the response depends on the phase of the initial breather as in Fig. 7. The inner product and associated distance are shown for two typical initial conditions (black and gray) with $c_3=0.142\,44$. Solid (respectively broken) curves indicate inner product (respectively distance to the scattor).

$$\text{distance} = \min_{\delta} \int_0^T |W(t) - W_{\text{BS}}(t+\delta)|^2 dt,$$

$$\text{inner product} = \frac{1}{T}\int_0^T \langle W(t) - W_{\text{BS}}(t+\delta), \Phi^* \rangle dt. \qquad (2)$$

Figure 6 shows how those quantities evolve with respect to

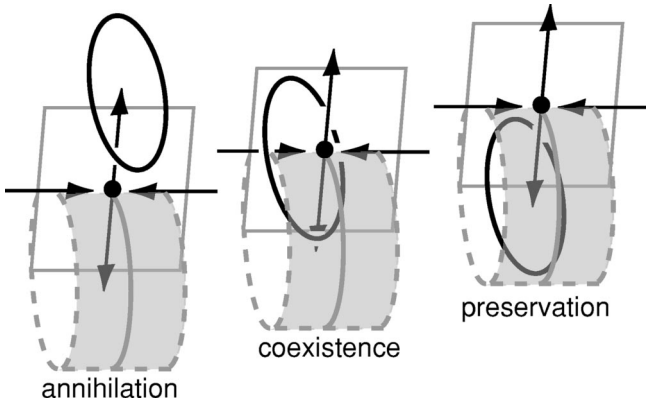

FIG. 7. Schematic picture of the relation for the plot of the profiles of the orbits right after collisions and the stable manifold of the time-periodic scattor of codim 1. The rectangle shows a Poincaré section of the scattor. The solid circle indicates the plot of profiles of the orbit as the collision-phase varies from 0 to 2π. It crosses the stable manifold of the scattor transversally as c_3 passes the transition point. Generically there is a nonempty interval of c_3 in which the circle belongs to both sides of the stable manifold of the scattor, which explains the outputs of Fig. 1(B)(c).

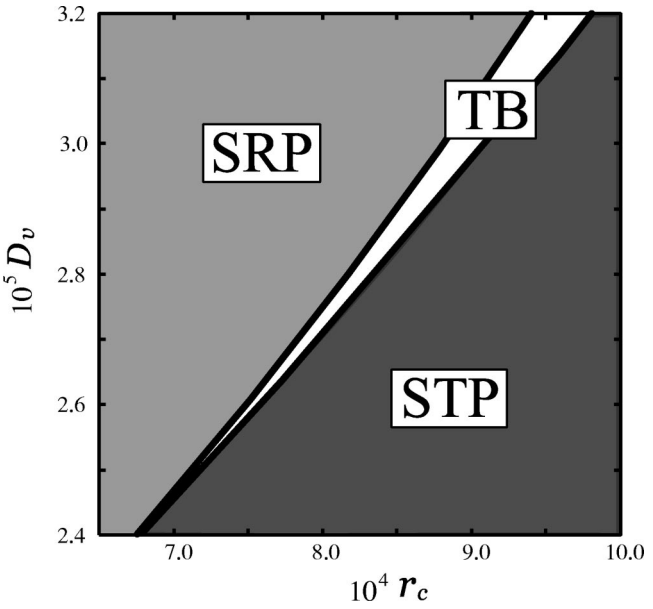

FIG. 8. Phase diagram in ($r_c\times10^4$, $D_v\times10^5$) space starting from a single pulse. SRP: self-replicating pattern. STP: stable traveling pulse. For parameters in SRP, each pulse undergoes backfiring.

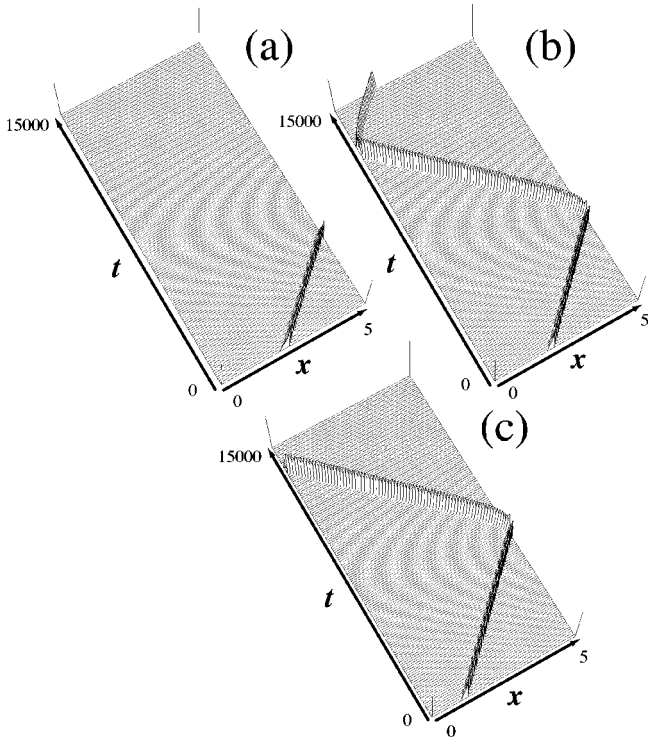

FIG. 9. Symmetric head-on collisions for the three-component system (3) (i.e., hitting the boundary with the Neumann condition). (a) Annihilation $D_v=2.6\times10^{-5}$, $r_c=7.52\times10^{-4}$. (b) Preservation $D_v=3.2\times10^{-5}$, $r_c=9.72\times10^{-4}$. (c) The output changes depending on the phase at collision: the first one is of preservation and the second one is of annihilation. $D_v=3.19\times10^{-5}$, $r_c=9.60\times10^{-4}$ Only u component is displayed here.

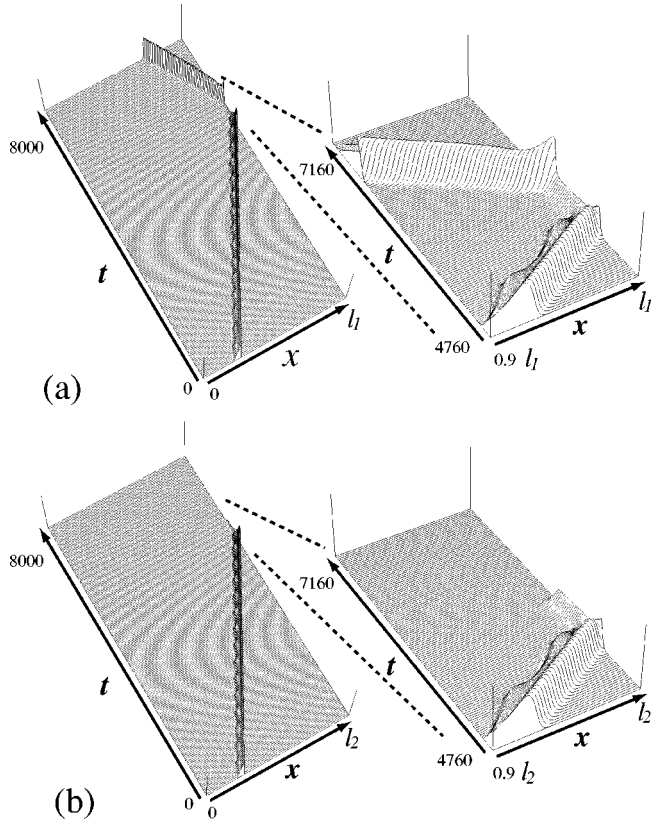

FIG. 10. The outputs depend on the phase at collision. The difference between (a) and (b) is the phase at collision. The phase is controlled by tuning the distance of initial position to the boundary. The orbits stay close to the scattor for certain time in both cases: (a) preservation, (b) annihilation. The output depends on the system size l_1 and l_2 where $l_1 \approx 4.77$ and l_2 is slightly larger than l_1. The number of spatial grids is 1.0×10^3.

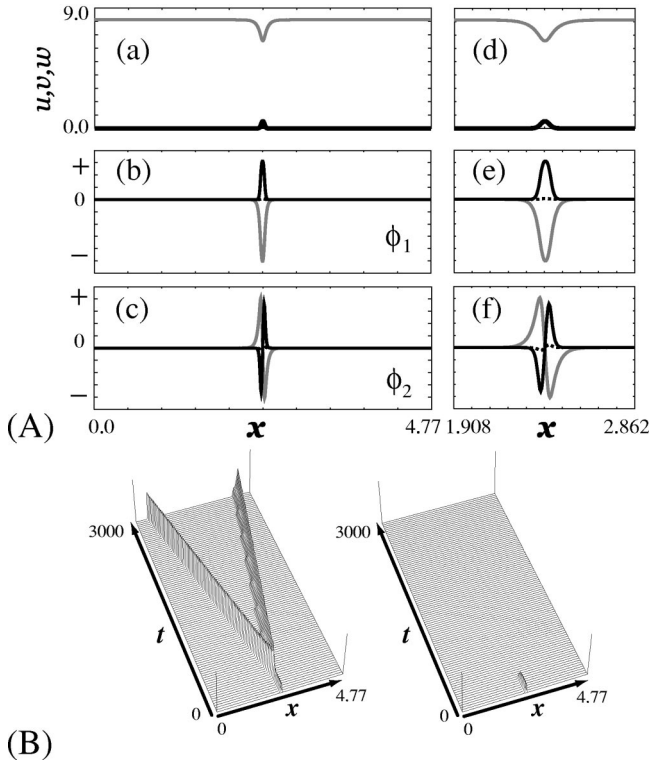

FIG. 11. (A)(a) The profile of the scattor of static type. The scattor is of codim 2. Note that the profile of w is exactly the same as that of u. The number of spatial grids is 1.0×10^3. (b),(c) The unstable eigenfunctions ϕ_1 and ϕ_2 are depicted. The associated eigenvalues are 0.046 360 78 and 0.014 041 54. (d)–(f) The magnified pictures of central parts of (a)–(c), respectively. The solid, gray, and dotted lines indicate u, v, and w components, respectively. (B) left (right) Outputs from the scattor. A small positive (negative) perturbation of ϕ_1 is added to the scattor.

time: The sign of the inner product is changed near the minimum distance point before and after the transition point $c_3 \approx 0.142\,429$, which implies the switching of the orbital behavior from one side to the other. If we plot the profiles of the orbit right after collision in the appropriate phase near the scattor, then it becomes a closed curve as the phase at collision varies from 0 to 2π, moreover the closed curve generically crosses the stable manifold of USP transversally as c_3 varies as shown in Fig. 7. The output after collision is therefore determined by looking at on which side of the stable manifold the closed curve belongs. In view of Fig. 7, it is clear that two different types of outputs come out depending on the phase. Accordingly, the coexistence of the annihilation and preservation for the fixed c_3 value as shown in Fig. 1(B)(c) is caused by the difference of phase at collision.

IV. SCATTORS FOR THE ACTIVATOR-SUBSTRATE-INHIBITOR SYSTEM

The scattor for the CGLE (1) turns out to be time periodic as was discussed in previous sections, however this is not always the case. In fact the following three-component system (3) has a TB in an appropriate parameter regime (Fig. 8):

$$u_t = D_u u_{xx} + \frac{su^2 v}{(s_b + s_c w)(1 + s_a u^2)} - r_a u,$$

$$v_t = D_v v_{xx} + b_b - \frac{su^2 v}{(s_b + s_c w)(1 + s_a u^2)} - r_b v,$$

$$w_t = r_c(u - w). \tag{3}$$

This model can be regarded as a 3×3 system by adding the effect of the inhibitor w to the 2×2 activator-substrate system such as the Gray-Scott model. For more details, see for instance Meinhardt [22]. We adopt two parameters D_v and r_c as bifurcation parameters. Note that steady states do not depend on r_c. Other parameters are fixed as $D_u = 1.0 \times 10^{-5}$, $r_a = 0.082$, $r_b = 0.0123$, $b_b = 0.1$, $s_a = 1.11$, $s_b = 1.55$, $s_c = 1.115$, $s = 0.08$. For numerical computation, we set to $\Delta x = 0.004$ and $\Delta t = 0.1$ unless otherwise said. Figure 9 shows three typical behaviors at symmetric collisions in TB regime of Fig. 8. Preservation (respectively annihilation) occurs in the right-upper (respectively left-lower) region of TB regime. In

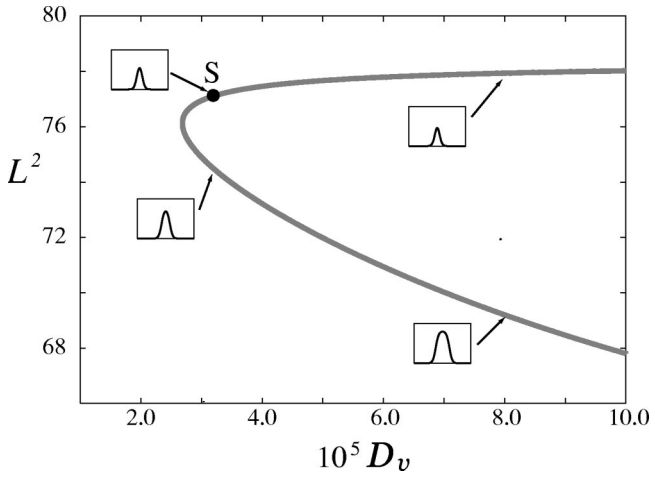

FIG. 12. Continuation of the scattor S corresponding to Fig. 11(A) with D_v being a bifurcation parameter and $r_c=9.6\times10^{-4}$. The branch turns back at a saddle-node (SN) point $D_v=2.682\,54\times10^{-5}$.

between those regimes, preservation and annihilation occur simultaneously as in Fig. 9(c) depending on the collision-phase similar to Fig. 1(B)(c). Taking a closer look at two collisions of Fig. 9(c), we see that the orbits become very close to a quasi-steady-state for certain time before preservation or annihilation as depicted in Fig. 10; in fact an unstable steady state can be found by the Newton method and it has two unstable eigenvalues as shown in Fig. 11(A) besides the translation zero eigenvalue. This steady state is deserved to be called a scattor, because it emits exactly the same outputs as observed in Fig. 10 (see Fig. 11) when it is perturbed along the first (symmetric) unstable direction [see Fig. 11(B)]. Note that Fig. 12 shows that the scattor S depends smoothly on D_v in a wider interval. It should be remarked that the scattor for Eq. (3) is not time periodic. The mechanism proposed for the CGLE remains valid without alteration; in particular, phase-dependent output originates from the intersecting manner between the stable manifold of the scattor and the loop structure of the profiles at collision.

V. CONCLUSION

Scattering phenomena of oscillatory-propagating pulses (TBs) are studied for the CGLE (1) and the three-component reaction diffusion system (3). The transition of input-output relation such as from annihilation to preservation can be explained from the scattor's viewpoint. The scattor for the CGLE (1) takes a form of unstable time-periodic solution, however this is not always the case for the three-component system (3) as shown in the preceding section. The solution profile right after collision is a function of the collision phase, and it makes a closed loop generically. This loop intersects transversally with the stable manifold of the scattor near the transition point of input-output relation, which causes the phase-dependent output. Such scattors can be found systematically by adopting a global bifurcation viewpoint with the aid of the path-tracking software such as AUTO. The origin of a diversity of input-output relations can be reduced to the local dynamics around scattors, in fact, when the orbit approaches a scattor right after collision, then it is sorted out along one of the unstable directions of it.

Here we focused on the symmetric head-on collision, i.e., hitting the boundary with Neumann condition. A collision process and the associated scattor correspond to the in-phase oscillations on a whole line. For asymmetric collisions, namely, the phases of two colliding TBs are different, the outputs become more complicated and the response of scattor for the asymmetric perturbations must be considered, which is a part of the ongoing project. Overall the response of scattors plays a pivotal role to understand the transient aspect of scattering dynamics in dissipative systems.

ACKNOWLEDGMENTS

This work was supported by the Grant-in-Aid for Scientific Research Grant No. (B)13440027 and for Exploratory Research Grant No. 14654018 and the 21st Century COE Program; Integrative Mathematical Sciences: Progress in Mathematics Motivated by Social and Natural Sciences.

[1] Y. Nishiura and D. Ueyama, Physica D **130**, 73 (1999).
[2] Y. Nishiura and D. Ueyama, Physica D **150**, 137 (2001).
[3] M. G. Zimmermann *et al.*, Physica D **110**, 92 (1997).
[4] V. Petrov, S. K. Scott, and K. Showalter, Philos. Trans. R. Soc. London, Ser. A **347**, 631 (1994).
[5] Y. Nishiura, *Far-from-Equilibrium Dynamics* (AMS, Providence, RI, 2002).
[6] K. Krischer and A. Mikhailov, Phys. Rev. Lett. **73**, 3165 (1994).
[7] S. Kawaguchi and M. Mimura, SIAM (Soc. Ind. Appl. Math.) J. Appl. Math. **59**, 920 (1999).
[8] M. Mimura and M. Nagayama, Chaos **7**, 817 (1997).
[9] Y. Astrov and H.-G. Purwin, Phys. Lett. A **283**, 349 (2001).
[10] M. Bode, A. W. Liehr, C. P. Schenk, and H.-G. Purwins, Physica D **161**, 45 (2002).
[11] M. Bär, M. Eiswirth, H.-H. Rotermund, and G. Ertl, Phys. Rev. Lett. **69**, 945 (1992).
[12] A. von Oertzen, A. S. Mikhailov, H. H. Rotermund, and G. Ertl, J. Phys. Chem. B **102**, 4966 (1998).
[13] P. Kolodner, Phys. Rev. A **44**, 6466 (1991).
[14] M. Argentina, P. Coullet, and L. Mahadevan, Phys. Rev. Lett. **79**, 2803 (1997).
[15] Y. Nishiura, T. Teramoto, and K.-I. Ueda, Phys. Rev. E **67**, 056210 (2003).
[16] Y. Nishiura, T. Teramoto, and K.-I. Ueda, Chaos **13**, 962 (2003).
[17] E. J. Doedel, A. R. Champneys, T. F. Fairgrieve, Y. A. Kuz-

netsov, B. Sandstede, and X. Wang, AUTO97, http://cmvl.cs.concordia.ca/auto, 1997.
[18] I. S. Aranson and L. Kramer, Rev. Mod. Phys. **74**, 99 (2002).
[19] P. Coullet, J. Lega, B. Houchmanzadeh, and J. Lajzerowicz, Phys. Rev. Lett. **65**, 1352 (1990).
[20] T. Ohta, J. Kiyose, and M. Mimura, J. Phys. Soc. Jpn. **66**, 1551 (1997).
[21] T. Mizuguchi and S. Sasa, Prog. Theor. Phys. **89**, 599 (1993).
[22] H. Meinhardt, *The Algorithmic Beauty of Sea Shells* (Springer-Verlag, Berlin, 1999).